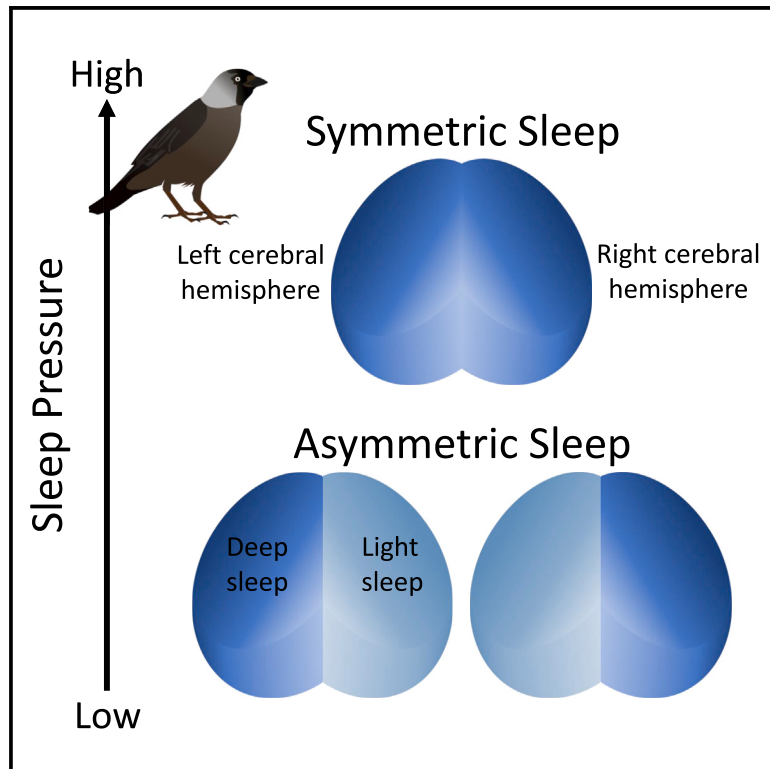


Current Biology

Sleep pressure causes birds to trade asymmetric sleep for symmetric sleep

Graphical abstract



Authors

Sjoerd J. van Hasselt,
Dolores Martinez-Gonzalez,
Gert-Jan Mekenkamp, ...,
Gabiël J.L. Beckers,
Niels C. Rattenborg, Peter Meerlo

Correspondence

niels.rattenborg@bi.mpg.de (N.C.R.),
p.meerlo@rug.nl (P.M.)

In brief

Avian non-REM sleep can occur symmetrically, with both cerebral hemispheres sleeping deeply, or asymmetrically, with one sleeping lighter than the other. van Hasselt et al. find that during periods of increased sleep need, birds sacrifice asymmetric sleep and the potential vigilance it provides to recover lost sleep through sleeping symmetrically.

Highlights

- High-density EEG shows local homeostatic responses to sleep loss in the avian brain
- Theta oscillations occur during non-REM sleep in non-hippocampal brain regions
- Non-REM sleep occurs symmetrically and asymmetrically between the hemispheres
- Asymmetric sleep is sacrificed for symmetric sleep when sleep pressure increases



Report

Sleep pressure causes birds to trade asymmetric sleep for symmetric sleep

Sjoerd J. van Hasselt,^{1,5} Dolores Martinez-Gonzalez,^{2,5} Gert-Jan Mekenkamp,¹ Alexei L. Vyssotski,³ Simon Verhulst,¹ Gabriël J.L. Beckers,⁴ Niels C. Rattenborg,^{2,6,*} and Peter Meerlo^{1,6,7,*}

¹Groningen Institute for Evolutionary Life Sciences, University of Groningen, Nijenborgh 79747 Groningen, the Netherlands

²Max Planck Institute for Biological Intelligence, Avian Sleep, Eberhard-Gwinner-Straße 5, 82319 Seewiesen, Germany

³Institute of Neuroinformatics, University of Zürich, Swiss Federal Institute of Technology (ETH) Zürich, Winterthurerstrasse 190, 8057 Zürich, Switzerland

⁴Experimental Psychology and Helmholtz Institute, Utrecht University, Yalelaan 2, 3584 CM Utrecht, the Netherlands

⁵These authors contributed equally

⁶These authors contributed equally

⁷Lead contact

*Correspondence: niels.rattenborg@bi.mpg.de (N.C.R.), p.meerlo@rug.nl (P.M.)

<https://doi.org/10.1016/j.cub.2025.03.008>

SUMMARY

Sleep is a dangerous part of an animal's life.^{1–3} Nonetheless, following sleep loss, mammals and birds sleep longer and deeper, as reflected by increased electroencephalogram (EEG) slow-wave activity (SWA; $\approx 1–5$ Hz spectral power) during non-rapid eye movement (NREM) sleep.^{4,5} Stimulating a brain region during wakefulness also causes that region to sleep deeper afterwards,^{6–9} indicating that NREM sleep is a local, homeostatically regulated process.^{10,11} Birds and some marine mammals can keep one eye open during NREM sleep,^{12,13} a behavior associated with lighter sleep or wakefulness in the hemisphere opposite the open eye—states called asymmetric and unihemispheric NREM sleep, respectively.^{13–23} Closure of both eyes is associated with symmetric NREM or REM sleep. Birds rely on asymmetric and unihemispheric sleep to stay safe.^{17,24,25} However, as sleeping deeply with only one hemisphere at a time increases the time required for both hemispheres to fulfill their need for NREM sleep, increased sleep pressure might cause birds to engage in symmetric sleep at the expense of asymmetric sleep.^{26,27} Using high-density EEG recordings of European jackdaws (*Coloeus monedula*), we investigated intra- and inter-hemispheric asymmetries during normal sleep and following sleep deprivation (SD). The proportion of asymmetric sleep was lower early in the sleep period and following SD—periods of increased sleep pressure. Our findings demonstrate a trade-off between the benefits of sleep and vigilance and indicate that a bird's utilization of asymmetric sleep is constrained by temporal dynamics in their need for sleep.

RESULTS

We studied jackdaws (family Corvidae) because their large corvid brain, relative to body mass, allowed for recording from several regions simultaneously. Corvids are also of interest due to their primate-like cognitive abilities^{28,29} and higher neuronal densities in their pallial analogs of the mammalian cortex.^{30,31} We used a wireless data logger to record from 28 equally spaced epidural electroencephalogram (EEG) electrodes that spanned the dorsal surface of the jackdaw brain (Figure 1A). The electrodes were placed over the following brain regions (STAR Methods): visual hyperpallium—a large structure involved in processing visual information received from the lateral geniculate nucleus,³² the hippocampal formation—involved in processing spatial information,³³ and the dorsal ventricular ridge (DVR)—a large, multi-modal sensory and high-order association area that includes a functional analog of the mammalian prefrontal cortex.³⁴ To detect head movements, the logger also recorded tri-axial acceleration (Figure 1B). Recordings were made during

three consecutive days (12:12 LD), consisting of a baseline night and day, followed by sleep deprivation (SD) during the first 4 or 8 h of the second night and recovery during the remainder of that night, the following day, and a second recovery night and day.

The spectral properties of the jackdaw's EEG were largely comparable to those reported in other birds.^{23,35–43} Non-rapid eye movement (NREM) sleep was characterized by increased slow-wave activity (SWA; peak 2–4 Hz) relative to wakefulness and REM sleep (Figure 1C). Consistent with other EEG studies of birds, and intra-cerebral and thalamic recordings in pigeons (*Columba livia*),⁴⁴ 12–15 Hz mammalian thalamo-cortical spindles were not observed in the power spectra or the raw recordings. However, unlike recordings in other bird species, a second peak occurred around 7 Hz, resulting from a distinct oscillation visible in the raw (e.g., Figure 1B, bottom plot) and filtered (Figure S1) EEG recordings. The two frequency peaks were evident at most recording sites but were strongest in the visual hyperpallium and DVR and lowest in the hippocampal formation of each



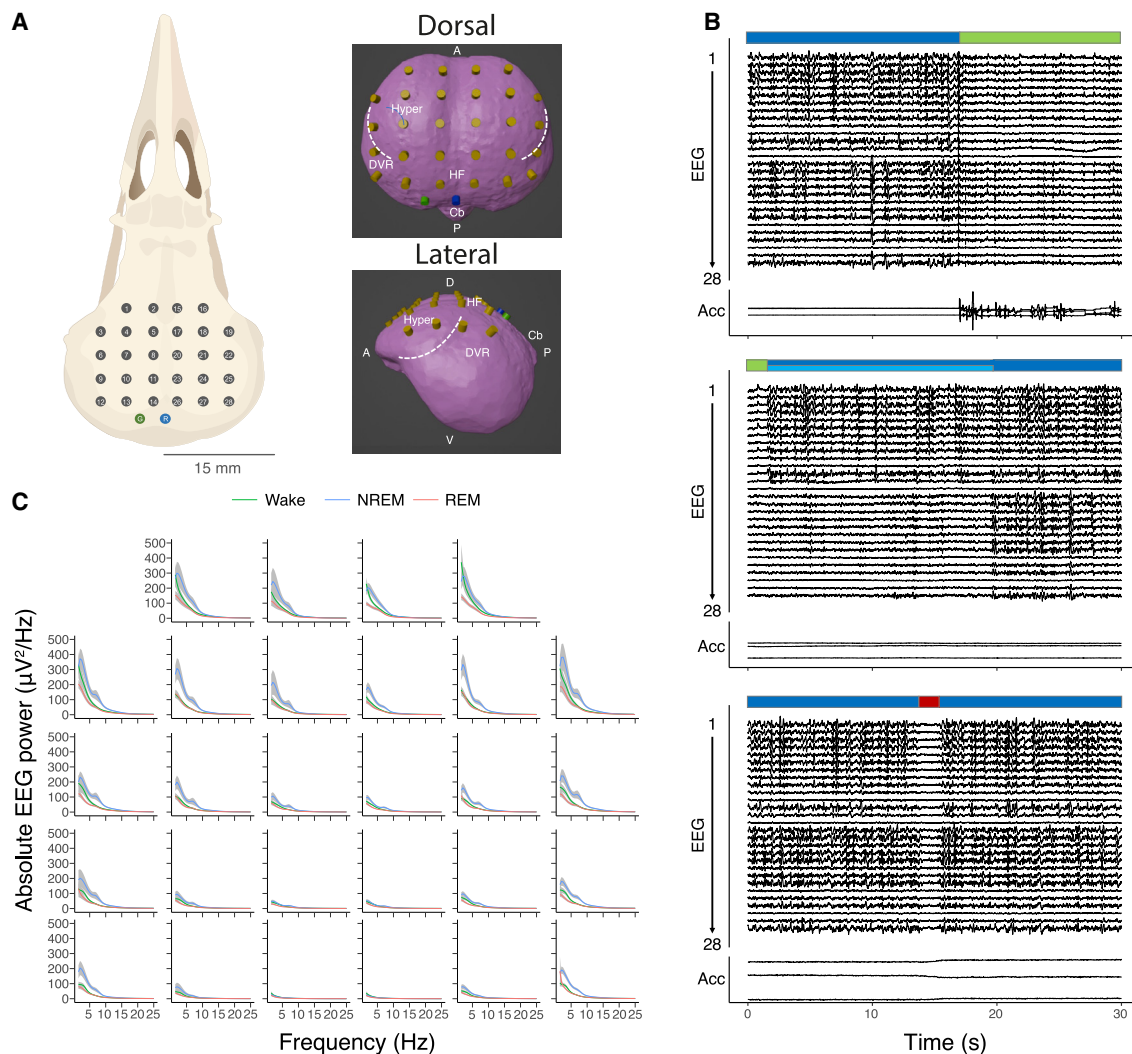


Figure 1. High-density EEG recordings in sleeping jackdaws

(A) Position of 28 epidural EEG electrodes on the skull (left) and over the brain (right). The 3D view of the brain was derived from a CT scan. The brain regions covered by the electrode array include the visual hyperpallium (Hyper), the dorsal ventricular ridge (DVR), and the hippocampal formation (HF) of each hemisphere. The dashed line represents the valleculla, a shallow suture demarcating the posterior-lateral boundary of the hyperpallium. A reference electrode (R, blue) was placed medially near the anterior cerebellum (Cb). A ground electrode (G, green) was placed posteriorly on the left hemisphere. The numbers correspond to the EEG channels in (B). (B) Three representative 30-s recordings of all 28 EEG channels and head acceleration (sway, surge, and heave) showing episodes of wake (green), symmetric NREM sleep (dark blue), asymmetric NREM sleep (dark + light blue), and REM sleep (red) (see also [Videos S1, S2, and S3](#)). The electrodes are arranged 1 (top)—28 (bottom) according to their position on the brain in (A). (C) Mean EEG power spectra for the three states (wake, NREM, and REM sleep) during a 24-h baseline day plotted for all electrodes arranged according to their position on the brain. The gray shaded area around the curves indicates SEM. Abbreviations: EEG, electroencephalogram; A, anterior; P, posterior; D, dorsal; V, ventral; Acc (acceleration).

See also [Figures S1 and S2](#) and [Videos S1, S2, and S3](#).

hemisphere. Although proximity to the reference electrode might have contributed to this lower power, medial electrodes farther from the reference had lower power than lateral electrodes closer to the reference (e.g., 8 vs. 12 and 20 vs. 28). SWA was greatest early in the night, whereas power around 7 Hz was greatest early and late in the night ([Figure S2](#)). NREM sleep occurred symmetrically, asymmetrically ([Figure 1B](#)), and uni-hemispherically. On a compressed timescale, NREM sleep EEG activity appeared synchronous within a hemisphere. However, when visualized as a slowed-down video, waves of activity usually emerged asynchronously within a hemisphere and appeared

to travel across the surface of a hemisphere, or even between hemispheres, in variable patterns ([Videos S1, S2, and S3](#)^{44,45}).

The baseline sleep patterns of jackdaws were similar to other diurnal birds.⁴⁶ The 24-h day consisted of $51.5\% \pm 0.4\%$ wakefulness, $39.8\% \pm 1.1\%$ NREM sleep, and $8.7\% \pm 1.1\%$ REM sleep, with sleep occurring mostly at night (dark phase: $75.3\% \pm 2.1\%$ NREM sleep and $17.2\% \pm 2.3\%$ REM sleep; light phase $4.3\% \pm 1.0\%$ NREM sleep and $0.14\% \pm 0.02\%$ REM sleep). REM sleep made up $18.6\% \pm 2.4\%$ of total night sleep time, $3.8\% \pm 0.7\%$ of total day sleep time, and $17.8\% \pm 2.3\%$ of total sleep time of a 24-h day. Across nights, the percentage of time spent in NREM

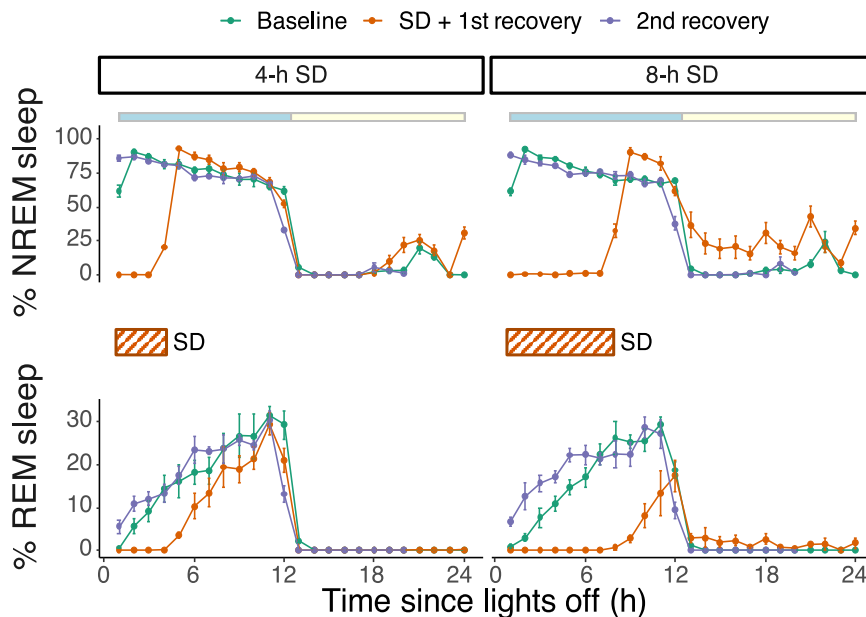


Figure 2. Impact of SD on NREM and REM sleep

The hourly percentages of NREM (top panels) and REM (bottom panels) sleep during the baseline day (green), the experimental day with SD and 1st recovery (orange), and 2nd recovery day (purple). The light:dark cycle is denoted by the yellow and blue bars on top, respectively. The orange hatched bars in the middle of the figure denote the SD period (4 and 8 h). After both SDs, the amount of NREM sleep increased during the remainder of the night. NREM sleep time remain elevated into the light phase only after 8-h SD. After 4-h SD there was no change in REM sleep time, whereas 8-h SD yielded an increase in REM sleep time during the light phase and 2nd recovery night. Data are plotted as mean \pm SEM. See also Figures S3 and S4.

and REM sleep decreased and increased, respectively ($p < 0.001$ for both NREM and REM sleep; Imer model; Figure 2). The mild stimulation used to prevent sleep was highly effective in keeping the birds awake during the 4- and 8-h SD. During the remainder of the night following SD, there was an increase in NREM sleep time that lasted 2 h after 4-h SD ($p < 0.05$; post hoc test after Imer model) and 3 h after 8-h SD ($p < 0.05$; post hoc test after Imer model). In addition, after 8-h SD, but not 4-h SD, NREM sleep increased during the subsequent light phase ($p < 0.01$; Imer model). REM sleep was suppressed during SD and remained reduced for 2 h after 4-h SD and 3 h after 8-h SD ($p < 0.05$; post hoc test after Imer model). Subsequently, there was no sign of REM sleep recovery after 4-h SD. In contrast, after 8-h SD, the birds had 1.6 h more REM sleep during the following light phase ($p < 0.001$; Imer model) and REM sleep remained elevated during the first 6 h of the 2nd recovery night ($p < 0.05$; post hoc test after Imer model). The increases in NREM and REM sleep time during the recovery phase did not fully compensate for the sleep lost during SD (Figure S3). Finally, 4- and 8-h SD caused a similar increase in NREM sleep bout duration from approximately 30 s on the baseline night to 130 s on the 1st recovery night ($p = 0.016$ and $p = 0.007$, for 4- and 8-h SD, respectively; post hoc test after Imer model; Figure S4); bout duration decreased to baseline values on the 2nd recovery night ($p = 0.012$ and $p = 0.001$, for 4- and 8-h SD, respectively; post hoc test after Imer model). As in other birds,⁴⁶ baseline nighttime bouts of REM sleep lasted approximately 6–8 s. The only significant change was an increase to 9 s between the 1st and 2nd recovery nights following 8-h SD ($p = 0.015$; post hoc test after Imer model) (Figure S4), when the delayed recovery of REM sleep was also observed.

Sleep loss caused an initial increase in NREM sleep EEG power that dissipated across the remainder of the 1st recovery night (Figure 3A; Figure S2). As described in previous studies of birds using a smaller number of electrodes, the increase in EEG power was bimodal across a broad range of frequencies.^{9,37,38,42,47} Compared with the same hour of the baseline night, power

increased across 1.5–20 Hz, with two distinct peaks between approximately 1.5–5.5 (i.e., SWA) and 7.5–18 Hz during the first hour of recovery sleep. The bimodal increase was present following 4- and 8-h SD at virtually all 28 electrodes, indicating a widespread response of the avian brain to SD (Figure 3B). Nonetheless, the magnitude of this response was largest in the visual hyperpallium and DVR, regions that also showed the greatest baseline EEG power (Figure 1C). The bimodal nature of the initial response to SD was attributable to a small or absent increase in EEG power around 7 Hz, the frequency band that showed a power peak during baseline NREM sleep (Figure 1C) early and late in the night (Figure S2A). In addition to the limited initial response in this frequency, during the last 1–2 h of the 1st recovery night, 7 Hz power decreased relative to the same hours of the baseline night (Figure 3A; Figure S2). Consequently, unlike the 1.5- to 5.5-Hz SWA and the 7.5- to 18-Hz band, which showed large increases early in the recovery night, SD caused a small or no increase in 7 Hz power early in the night and suppressed it late in the night.

The bimodal response to SD was evident in all electrodes, but the relative magnitude of the increase in the two frequency bands varied by region. To quantify local variation in the EEG response to SD, we calculated the area under the curve (AUC) for the 1.5- to 5.5-Hz SWA and the 7.5- to 18-Hz band during the first hour of recovery (Figure 3B). SWA showed the greatest increase in the DVR ($p < 0.001$; Imer model; Figure 3C). In contrast, power in the 7.5- to 18-Hz band increased the most in the visual hyperpallium ($p < 0.001$; Imer model; Figure 3D). As with the regional differences in absolute power, these differences were largely mirrored between the two hemispheres. For both frequency ranges, the increase in AUC was slightly higher after 4-h SD compared with 8-h SD (SWA: $p = 0.04$; 7.5–18 Hz band: $p = 0.009$; Imer model). Consequently, unlike the time spent in NREM and REM sleep, EEG power did not show a dose-dependent increase in response to SD.

In addition to impacting intra-hemispheric EEG power asymmetries, SD also influenced inter-hemispheric asymmetry. For all epochs of NREM sleep, on each night, we calculated the inter-hemispheric asymmetry index (AI) between the left and right

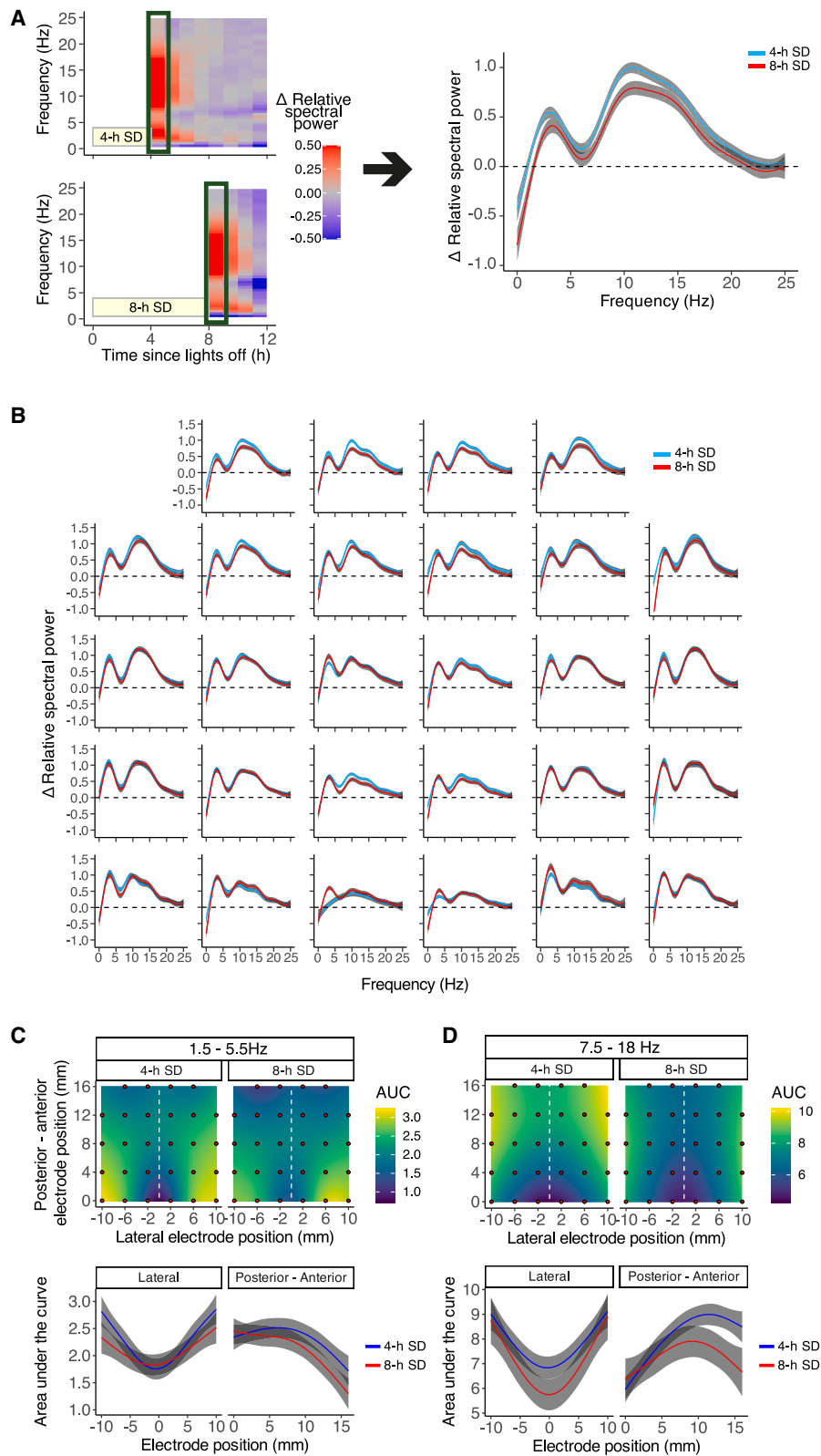


Figure 3. Bimodal NREM sleep EEG response to SD by brain region

As shown in (A) for the anterior left electrode, the change in relative EEG power (0.5–25 Hz) after 4-h (blue) and 8-h (red) SD was extracted for the first hour of recovery, when the response was maximal, and plotted for each electrode according to its position on the brain (B). For both SDs, there was an immediate increase in spectral

(legend continued on next page)

hemispheres for 1.5–5.5 Hz SWA (STAR Methods).^{25,48} In addition, we calculated the AI for the 7.5- to 18-Hz band that also responded to SD. To explore potential regional differences in inter-hemispheric asymmetries,⁴⁹ we calculated the AI for 3 inter-hemispheric pairs of electrodes spaced 12 mm apart along a left to right axis (6 mm lateral of the midline) and 8 mm apart along the anterior-posterior axis (Figure 4). The electrode pairs corresponded to the anterior visual hyperpallium (anterior pair), posterior visual hyperpallium (middle pair), and hippocampal formation (posterior pair). For all three electrode pairs, the majority of epochs had AI values for 1.5–5.5 Hz SWA, falling in the category of symmetric NREM sleep (Figure 4A). The number of epochs that fulfilled the criteria for unihemispheric sleep was low for all three electrode pairs and conditions (less than 0.1% in each case), but a substantial portion of the epochs fell in the category of asymmetric NREM sleep (4-h SD baseline; anterior pair: $18.4\% \pm 1.8\%$, middle pair: $18.3\% \pm 2.3\%$, posterior pair: $31\% \pm 5.7\%$; 8-h SD baseline; anterior pair: $17.6\% \pm 1.7\%$, middle pair: $19.3\% \pm 2.1\%$, posterior pair: $30.7\% \pm 4.3\%$). The AI for 7.5–18 Hz power showed largely similar distributions (Figure S5A). For the posterior visual hyperpallium, the distribution in both frequency bands was skewed to the right for all 3 nights (more epochs with higher EEG power in the left hemisphere). And, the distribution of asymmetry values for the hippocampal formation was skewed to the left for all 3 nights and both frequency bands (more epochs with higher EEG power in the right hemisphere).

We next investigated whether homeostatic sleep pressure impacted the occurrence of asymmetric NREM sleep. Due to the low amount of unihemispheric NREM sleep, we combined unihemispheric and asymmetric NREM sleep and plotted the proportion of NREM sleep with asymmetry values exceeding the threshold for asymmetric NREM sleep. In general, EEG asymmetry in NREM sleep increased along the anterior-posterior axis ($p < 0.001$; lmer model; Figure 4, Figure S5B). The asymmetry values for the 7.5- to 18-Hz band were largely constant across the night and unaffected by SD (Figure S5B). In contrast, asymmetry values for the 1.5- to 5.5-Hz SWA in the visual hyperpallium (anterior and middle pairs) significantly increased across the night ($p < 0.05$; post hoc test after lmer model; Figure 4B). In addition, the asymmetry values for SWA were reduced during the initial hours following 4- and 8-h SD in the anterior visual hyperpallium and, to some extent, after 8-h SD in the posterior visual hyperpallium ($p < 0.05$; post hoc test after lmer model; Figure 4B). Collectively, this suggests that during periods with elevated sleep pressure (i.e., at the beginning of nighttime sleep after a day spent mostly awake or after extending wakefulness by 4 or 8 h), sleep in the visual hyperpallium is more symmetric.

DISCUSSION

EEG activity and its response to SD varied across the surface of the brain. The hippocampal formation showed the lowest EEG

power during baseline NREM sleep and the smallest increase during recovery from SD. The hippocampal formation—a relatively thin structure resting between the dura and lateral ventricle in birds—might lack the capacity to generate the higher voltages observed in other brain regions. Electrodes that recorded greater EEG power were over the visual hyperpallium—a primary visual area—and the DVR. As both regions are comparatively thick, this might explain the stronger signals in these areas. Alternatively, these regional differences in EEG voltage might reflect intrinsic neurophysiological and functional properties of these regions.

Jackdaws exhibited a distinct 7-Hz oscillation during NREM sleep not found in other birds. Although the avian EEG, in general, includes power in a wide range of frequencies, including 7 Hz, with a peak around 2–4 Hz during NREM sleep, a distinct secondary 7-Hz peak in absolute power has only been found in jackdaws.^{23,35–43} Given the widespread distribution of the 7-Hz power peak, including regions (e.g., visual hyperpallium) targeted in previous studies, it seems unlikely that a similar oscillation was missed in other birds. Consequently, the 7-Hz oscillation might be unique to jackdaws or, at the very least, more developed in this species. This might be mechanistically and functionally linked to the large brains with high neuronal densities^{30,31} and associated complex cognitive abilities that evolved in corvids.²⁸ A similar oscillation, albeit occurring in the rodent hippocampus primarily during REM sleep, called theta, has been implicated in memory consolidation.^{50,51} Despite the different sleep states and brain regions involved, 7-Hz oscillations might serve a similar function in jackdaw brains.⁵²

The bimodal increase in EEG power observed in jackdaws following SD has been found in several species of birds.^{9,37,38,42,47} Our high-density EEG recordings indicate that much of the dorsal surface of the avian brain responds in this manner. The increase in SWA after 4-h SD is consistent with studies of sleep homeostasis in mammals,⁴ wherein SWA is thought to reflect sleep pressure and to play a role in synaptic homeostasis and memory processing.^{10,53} However, the absence of an even greater increase following 8-h SD is inconsistent with findings in mammals and suggests that the capacity of the avian brain to increase SWA during NREM sleep is limited. To varying degrees, a similar bimodal increase in EEG power, with a dip around 6–8 Hz, during recovery from SD has also been observed in rats,⁵⁴ mice,⁵⁵ Syrian hamsters,⁵⁶ and rabbits.⁵⁷ The reason for this dip, as well as the mechanisms and functions of the increase in higher frequencies, is unknown in mammals and birds. The finding that power around 7 Hz increases the least following SD in birds and several mammals suggests that the differential regulation of this frequency band is a common feature of NREM sleep in birds and mammals, despite their differences in brain organization.

Jackdaws exhibited region-specific differences in the lateralization of asymmetric sleep. In the anterior visual hyperpallium,

power around two distinct peaks (approximately 1.5–5.5 Hz SWA and 7.5–18 Hz). To investigate regional- and frequency-specific differences in this response, we plotted the area under the curve (AUC) for 1.5–5.5 Hz SWA (C) and 7.5–18 Hz (D). The red dots in the top panels of (C) and (D) reflect the electrode positions. The heatmaps show the AUC based on a GAM model. The AUC for 1.5–5.5 Hz SWA increased to a greater extent in the posterior-lateral electrodes (DVR), whereas the AUC for 7.5–18 Hz increased to a greater extent in the anterior-lateral electrodes (visual hyperpallium). The most-lateral electrodes showed the greatest increase in the AUC for both frequency bands (bottom plots and C and D). The gray shaded areas around the curves in A–D indicate mean \pm CI (95%). See also Figure S2.

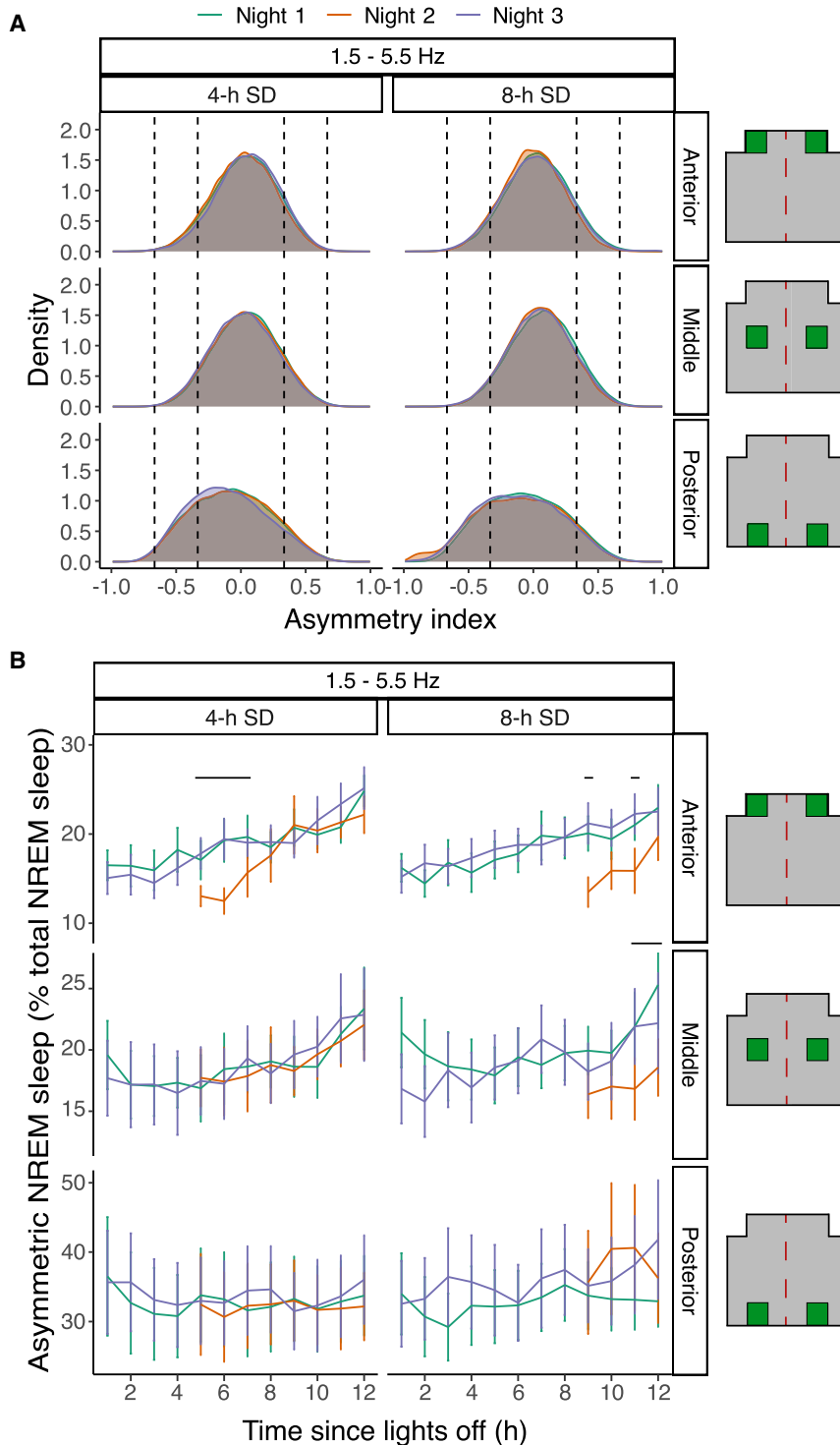


Figure 4. Sleep pressure decreases asymmetric sleep

(A) Distribution of the asymmetry index (AI) values for 1.5–5.5 Hz SWA for three electrode pairs (green in right electrode plots), during the baseline night (night 1, green), the 1st recovery night (night 2, orange), and the 2nd recovery night (night 3, purple) following 4- and 8-h SD. The dashed vertical lines indicate the thresholds for classifying NREM sleep as symmetric ($-0.33 < AI < 0.33$), asymmetric ($0.33 < AI < 0.67$ or $-0.33 > AI > -0.67$), and unihemispheric ($-0.67 > AI > 0.67$). The most prevalent form of NREM sleep was symmetric, followed by asymmetric, with only a small (<0.1%) proportion being unihemispheric.

(B) The hourly proportion of NREM sleep consisting of asymmetric NREM sleep during the 3 nights. Because the amount of unihemispheric NREM sleep was minimal, for this plot, unihemispheric and asymmetric NREM sleep epochs were grouped together as “asymmetric sleep.” Across the baseline nights, there was a significant increase in the proportion of asymmetric episodes in the anterior and posterior visual hyperpallium (anterior and medial pairs; $p < 0.001$; lmer model). This pattern was not detected in the hippocampal formation (posterior pair; $p = 0.1$; lmer model). The proportion of asymmetric NREM sleep was reduced in the anterior visual hyperpallium after 4- and 8-h SD and in the posterior hyperpallium after 8-h SD ($p < 0.05$; post hoc test after lmer model; black horizontal line in the graph denotes the statistical differences between night 1 and night 2). Data are plotted as mean \pm SEM. See also Figure S5.

the likelihood of the left or right sides sleeping deeper was similar. However, in the posterior visual hyperpallium, the right side was more likely to sleep deeper, whereas in the hippocampal formation it was the left side. This might be linked to functional lateralization in the brain,⁵⁸ which can influence hemispheric sleep in birds.^{59,60} Specifically, functional lateralization in the avian visual system⁶¹ and hippocampal formation^{62–65}

might explain the lateralization in sleep EEG that we found. As avian sleep is locally regulated in a use-dependent manner,⁹ more sleep in these regions could be a response to greater waking brain use. Several EEG studies of mammals and birds revealed shifts in the ratio of asymmetric to symmetric NREM sleep in response to changing ecological circumstances. Mallards (*Anas platyrhynchos*) switch from primarily engaging in symmetric NREM sleep when positioned safely in the center of a group to engaging in proportionately more asymmetric NREM sleep when vulnerable at the edge of a group.²⁴ Great frigatebirds engage in proportionately more asymmetric and unihemispheric NREM sleep in flight when compared with sleep on land.²⁵ Northern fur seals (*Callorhinus ursinus*) sleep primarily unihemispherically while in the water but symmetrically on land.⁶⁶ Finally, even though humans do not sleep with one eye open, NREM sleep intensity, based on EEG activity and responsiveness to sounds presented to the contralateral ear, is lower in certain regions of the left hemisphere on the first night sleeping in an unfamiliar environment; on

the second night, both hemispheres sleep deeply.⁶⁷ However, it is unclear whether these increases in symmetry reflect a homeostatic response to prior sleep loss, changes in perceived safety, a response to switching from the air to land in frigatebirds, or changes in activity and thermoregulation linked to switching from the water to land in fur seals.⁶⁶ Through conducting total SD in an otherwise unchanging environment, we demonstrate that increased sleep pressure causes birds to sacrifice asymmetric sleep to fulfill their need for sleep more efficiently through sleeping symmetrically. Although eye state and vigilance were not measured in this study, by sleeping symmetrically, sleepy jackdaws might sacrifice the visual or acoustic vigilance afforded by sleeping asymmetrically.

RESOURCE AVAILABILITY

Lead contact

Requests for further information and resources should be directed to, and will be fulfilled by, the lead contact, Peter Meerlo (p.meerlo@rug.nl).

Materials availability

This study did not generate new unique reagents.

Data and code availability

Requests for further information on raw data and R-scripts should be directed to, and will be fulfilled by, the [lead contact](#), Peter Meerlo (p.meerlo@rug.nl).

ACKNOWLEDGMENTS

This study was supported by a grant from the Dutch Research Council (OCENW.KLEIN.240) and an Adaptive Life Program scholarship from the Groningen Institute for Evolutionary Life Sciences at the University of Groningen to P.M. D.M.-G. and N.C.R. were supported by the Max Planck Society.

AUTHOR CONTRIBUTIONS

N.C.R., P.M., and S.J.v.H. conceived the study. S.V. coordinated the capture and maintenance of the jackdaws. S.J.v.H. and G.-J.M. hand-raised the jackdaws and conducted the experiments. S.J.v.H., N.C.R., and G.-J.M. performed the surgeries. D.M.-G. scored the sleep states. S.J.v.H. performed the statistical analyses. G.J.L.B. contributed to the signal analysis of the EEG and created the videos. A.L.V. developed neurologgers and participated in data collection. S.J.v.H., P.M., and N.C.R. wrote the manuscript with input from all coauthors.

DECLARATION OF INTERESTS

The authors declare no competing interests.

STAR★METHODS

Detailed methods are provided in the online version of this paper and include the following:

- KEY RESOURCES TABLE
- EXPERIMENTAL MODEL AND STUDY PARTICIPANT DETAILS
- METHOD DETAILS
 - Surgery
 - Sleep recordings
- QUANTIFICATION AND STATISTICAL ANALYSIS
 - Data analyses
 - Statistics

SUPPLEMENTAL INFORMATION

Supplemental information can be found online at <https://doi.org/10.1016/j.cub.2025.03.008>.

Received: December 17, 2024

Revised: February 14, 2025

Accepted: March 6, 2025

Published: March 31, 2025

REFERENCES

1. Rattenborg, N.C. (2024). Sleep is dangerous: historic hunting targeting fur seals sleeping unihemispherically at sea. *Sleep* 47, zsae026. <https://doi.org/10.1093/sleep/zsae026>.
2. Lima, S.L., Rattenborg, N.C., Lesku, J.A., and Amlaner, C.J. (2005). Sleeping under the risk of predation. *Anim. Behav.* 70, 723–736. <https://doi.org/10.1016/j.anbehav.2005.01.008>.
3. Ferretti, A., Rattenborg, N.C., Ruf, T., McWilliams, S.R., Cardinale, M., and Fusani, L. (2019). Sleeping unsafely tucked in to conserve energy in a nocturnal migratory songbird. *Curr. Biol.* 29, 2766–2772.e4. <https://doi.org/10.1016/j.cub.2019.07.028>.
4. Deboer, T. (2015). Behavioral and electrophysiological correlates of sleep and sleep homeostasis. In *Current Topics in Behavioral Neurosciences*, 25 (Springer), pp. 1–24. https://doi.org/10.1007/7854_2013_248.
5. Rattenborg, N.C., Martinez-Gonzalez, D., and Lesku, J.A. (2009). Avian sleep homeostasis: Convergent evolution of complex brains, cognition and sleep functions in mammals and birds. *Neurosci. Biobehav. Rev.* 33, 253–270. <https://doi.org/10.1016/j.neubiorev.2008.08.010>.
6. Kattler, H., Dijk, D.J., and Borbély, A.A. (1994). Effect of unilateral somatosensory stimulation prior to sleep on the sleep EEG in humans. *J. Sleep Res.* 3, 159–164. <https://doi.org/10.1111/j.1365-2869.1994.tb00123.x>.
7. Vyazovskiy, V., Borbély, A.A., and Tobler, I. (2000). Unilateral vibrissae stimulation during waking induces interhemispheric EEG asymmetry during subsequent sleep in the rat. *J. Sleep Res.* 9, 367–371. <https://doi.org/10.1046/j.1365-2869.2000.00230.x>.
8. Huber, R., Ghilardi, M.F., Massimini, M., and Tononi, G. (2004). Local sleep and learning. *Nature* 430, 78–81. <https://doi.org/10.1038/nature02663>.
9. Lesku, J.A., Vyssotski, A.L., Martinez-Gonzalez, D., Wilzeck, C., and Rattenborg, N.C. (2011). Local sleep homeostasis in the avian brain: convergence of sleep function in mammals and birds? *Proc. Biol. Sci.* 278, 2419–2428. <https://doi.org/10.1098/rspb.2010.2316>.
10. Tononi, G., and Cirelli, C. (2014). Sleep and the price of plasticity: from synaptic and cellular homeostasis to memory consolidation and integration. *Neuron* 81, 12–34. <https://doi.org/10.1016/j.neuron.2013.12.025>.
11. Nir, Y., and de Lecea, L. (2023). Sleep and vigilance states: embracing spatiotemporal dynamics. *Neuron* 111, 1998–2011. <https://doi.org/10.1016/j.neuron.2023.04.012>.
12. Lyamin, O.I., and Siegel, J.M. (2019). Sleep in Aquatic Mammals. In *Handbook of Behavioral Neuroscience*, 30, H.C. Dringenberg, ed. (Elsevier), pp. 375–393. <https://doi.org/10.1016/B978-0-12-813743-7.00025-6>.
13. Rattenborg, N.C., Van Der Meij, J., Beckers, G.J.L., and Lesku, J.A. (2019). Local aspects of avian non-rem and rem sleep. *Front. Neurosci.* 13, 567. <https://doi.org/10.3389/fnins.2019.00567>.
14. Peters, J., Vonderahe, A., and Schmid, D. (1965). Onset of cerebral electrical activity associated with behavioral sleep and attention in the developing chick. *J. Exp. Zool.* 160, 255–261. <https://doi.org/10.1002/jez.1401600303>.
15. Tarao, M., and Ookawa, T. (1969). On the electroencephalogram in the unilateral optic enucleated chick. *Poult. Sci.* 48, 1516–1517. <https://doi.org/10.3382/ps.0481516>.

16. Rattenborg, N.C., Lima, S.L., and Amlaner, C.J. (1999). Facultative control of avian unihemispheric sleep under the risk of predation. *Behav. Brain Res.* *105*, 163–172. [https://doi.org/10.1016/S0166-4328\(99\)00070-4](https://doi.org/10.1016/S0166-4328(99)00070-4).
17. Rattenborg, N.C., Amlaner, C.J., and Lima, S.L. (2001). Unilateral eye closure and interhemispheric EEG asymmetry during sleep in the pigeon (*Columba livia*). *Brain Behav. Evol.* *58*, 323–332. <https://doi.org/10.1159/000057573>.
18. Fuchs, T., Maury, D., Moore, F.R., and Bingman, V.P. (2009). Daytime micro-naps in a nocturnal migrant: an EEG analysis. *Biol. Lett.* *5*, 77–80. <https://doi.org/10.1098/rsbl.2008.0405>.
19. Kendall-Bar, J.M., Vyssotski, A.L., Mukhametov, L.M., Siegel, J.M., and Lyamin, O.I. (2019). Eye state asymmetry during aquatic unihemispheric slow wave sleep in northern fur seals (*Callorhinus ursinus*). *PLOS One* *14*, e0217025.
20. Libourel, P.A., Lee, W.Y., Achin, I., Chung, H., Kim, J., Massot, B., and Rattenborg, N.C. (2023). Nesting chinstrap penguins accrue large quantities of sleep through seconds-long microsleeps. *Science* *382*, 1026–1031. <https://doi.org/10.1126/science.adh0771>.
21. Lyamin, O.I., Mukhametov, L.M., Siegel, J.M., Nazarenko, E.A., Polyakova, I.G., and Shpak, O.V. (2002). Unihemispheric slow wave sleep and the state of the eyes in a white whale. *Behav. Brain Res.* *129*, 125–129. [https://doi.org/10.1016/S0166-4328\(01\)00346-1](https://doi.org/10.1016/S0166-4328(01)00346-1).
22. Ball, N.J., Amlaner, C.J., Shaffery, J.P., and Opp, M.R. (1988). Asynchronous eye-closure and unihemispheric quiet sleep of birds. In *Sleep*, 86, W.P. Koella, F. Obál, H. Schulz, and P. Visser, eds. (Gustav Fischer Verlag), pp. 151–153.
23. Low, P.S., Shank, S.S., Sejnowski, T.J., and Margoliash, D. (2008). Mammalian-like features of sleep structure in zebra finches. *Proc. Natl. Acad. Sci. USA* *105*, 9081–9086. <https://doi.org/10.1073/pnas.0703452105>.
24. Rattenborg, N.C., Lima, S.L., and Amlaner, C.J. (1999). Half-awake to the risk of predation. *Nature* *397*, 397–398. <https://doi.org/10.1038/17037>.
25. Rattenborg, N.C., Voirin, B., Cruz, S.M., Tisdale, R., Dell’Omo, G., Lipp, H.P., Wikelski, M., and Vyssotski, A.L. (2016). Evidence that birds sleep in mid-flight. *Nat. Commun.* *7*, 12468. <https://doi.org/10.1038/ncomms12468>.
26. Boerema, A.S., Riedstra, B., and Strijkstra, A.M. (2003). Decrease in monocular sleep after sleep deprivation in the domestic chicken. *Behaviour* *140*, 1415–1420. <https://doi.org/10.1163/156853903771980657>.
27. Lyamin, O.I., Kosenko, P.O., Lapierre, J.L., Mukhametov, L.M., and Siegel, J.M. (2008). Fur seals display a strong drive for bilateral slow-wave sleep while on land. *J. Neurosci.* *28*, 12614–12621. <https://doi.org/10.1523/JNEUROSCI.2306-08.2008>.
28. Clayton, N.S., and Emery, N.J. (2015). Avian models for human cognitive neuroscience: a proposal. *Neuron* *86*, 1330–1342. <https://doi.org/10.1016/j.neuron.2015.04.024>.
29. Nieder, A., Wagener, L., and Rinnert, P. (2020). A neural correlate of sensory consciousness in a corvid bird. *Science* *369*, 1626–1629. <https://doi.org/10.1126/science.abb1447>.
30. Olkowicz, S., Kocourek, M., Lučan, R.K., Porteš, M., Fitch, W.T., Herculano-Houzel, S., and Němec, P. (2016). Birds have primate-like numbers of neurons in the forebrain. *Proc. Natl. Acad. Sci. USA* *113*, 7255–7260. <https://doi.org/10.1073/pnas.1517131113>.
31. Kverková, K., Marhounová, L., Polonyiová, A., Kocourek, M., Zhang, Y., Olkowicz, S., Straková, B., Pavelková, Z., Vodička, R., Frynta, D., et al. (2022). The evolution of brain neuron numbers in amniotes. *Proc. Natl. Acad. Sci. USA* *119*, e2121624119. <https://doi.org/10.1073/pnas.2121624119>.
32. Stacho, M., Herold, C., Rook, N., Wagner, H., Axer, M., Amunts, K., and Güntürkün, O. (2020). A cortex-like canonical circuit in the avian forebrain. *Science* *369*, eabc5534. <https://doi.org/10.1126/science.abc5534>.
33. Madison, F.N., Bingman, V.P., Smulders, T.V., and Lattin, C.R. (2024). A bird’s eye view of the hippocampus beyond space: behavioral, neuroanatomical, and neuroendocrine perspectives. *Horm. Behav.* *157*, 105451. <https://doi.org/10.1016/j.yhbeh.2023.105451>.
34. Güntürkün, O., Pusch, R., and Rose, J. (2024). Why birds are smart. *Trends Cogn. Sci.* *28*, 197–209. <https://doi.org/10.1016/j.tics.2023.11.002>.
35. Tobler, I., and Borbély, A.A. (1988). Sleep and EEG spectra in the pigeon (*Columba livia*) under baseline conditions and after sleep deprivation. *J. Comp. Physiol.* *163*, 729–738. <https://doi.org/10.1007/BF00604050>.
36. Rattenborg, N.C., Mandt, B.H., Obermeyer, W.H., Winsauer, P.J., Huber, R., Wikelski, M., and Benca, R.M. (2004). Migratory sleeplessness in the white-crowned sparrow (*Zonotrichia leucophrys gambelii*). *PLOS Biol.* *2*, E212. <https://doi.org/10.1371/journal.pbio.0020212>.
37. Jones, S.G., Vyazovskiy, V.V., Cirelli, C., Tononi, G., and Benca, R.M. (2008). Homeostatic regulation of sleep in the white-crowned sparrow (*Zonotrichia leucophrys gambelii*). *BMC Neurosci.* *9*, 47. <https://doi.org/10.1186/1471-2202-9-47>.
38. Martinez-Gonzalez, D., Lesku, J.A., and Rattenborg, N.C. (2008). Increased EEG spectral power density during sleep following short-term sleep deprivation in pigeons (*Columba livia*): evidence for avian sleep homeostasis. *J. Sleep Res.* *17*, 140–153. <https://doi.org/10.1111/j.1365-2869.2008.00636.x>.
39. Scriba, M.F., Ducrest, A.L., Henry, I., Vyssotski, A.L., Rattenborg, N.C., and Roulin, A. (2013). Linking melanism to brain development: expression of a melanism-related gene in barn owl feather follicles covaries with sleep ontogeny. *Front. Zool.* *10*, 42. <https://doi.org/10.1186/1742-9994-10-42>.
40. Tisdale, R.K., Vyssotski, A.L., Lesku, J.A., and Rattenborg, N.C. (2017). Sleep-Related Electrophysiology and behavior of tinamous (*Eudromia elegans*): tinamous do not sleep like ostriches. *Brain Behav. Evol.* *89*, 249–261. <https://doi.org/10.1159/000475590>.
41. Canavan, S.V., and Margoliash, D. (2020). Budgerigars have complex sleep structure similar to that of mammals. *PLOS Biol.* *18*, e3000929. <https://doi.org/10.1371/journal.pbio.3000929>.
42. Van Hasselt, S.J., Rusche, M., Vyssotski, A.L., Verhulst, S., Rattenborg, N.C., and Meerlo, P. (2020). The European starling (*Sturnus vulgaris*) shows signs of NREM sleep homeostasis but has very little REM sleep and no REM sleep homeostasis. *Sleep* *43*, zsz311. <https://doi.org/10.1093/sleep/zsz311>.
43. Lyamin, O.I., Kibalnikov, A.S., and Siegel, J.M. (2021). Sleep in ostrich chicks (*Struthio camelus*). *Sleep* *44*, zsa259. <https://doi.org/10.1093/sleep/zsa259>.
44. Van Der Meij, J., Martinez-Gonzalez, D., Beckers, G.J.L., and Rattenborg, N.C. (2019). Intra-“cortical” activity during avian non-REM and REM sleep: variant and invariant traits between birds and mammals. *Sleep* *42*. <https://doi.org/10.1093/sleep/zsy230>.
45. Beckers, G.J.L., van der Meij, J., Lesku, J.A., and Rattenborg, N.C. (2014). Plumes of neuronal activity propagate in three dimensions through the nuclear avian brain. *BMC Biol.* *12*, 16. <https://doi.org/10.1186/1741-7007-12-16>.
46. Rattenborg, N.C., Lesku, J.A., and Libourel, P.-A. (2022). Sleep in Nonmammalian Vertebrates. In *Principles and Practices of Sleep Medicine 7e*, M.H. Kryger, T. Roth, C.A. Goldstein, and W.C. Dement, eds. (Elsevier), pp. 106–120.
47. Johnsson, R.D., Connelly, F., Vyssotski, A.L., Roth, T.C., and Lesku, J.A. (2022). Homeostatic regulation of NREM sleep, but not REM sleep, in Australian magpies. *Sleep* *45*, zsab218. <https://doi.org/10.1093/sleep/zsab218>.
48. Lyamin, O.I., Lapierre, J.L., Kosenko, P.O., Kodama, T., Bhagwandin, A., Korneva, S.M., Peever, J.H., Mukhametov, L.M., and Siegel, J.M. (2016). Monoamine release during unihemispheric sleep and unihemispheric waking in the fur seal. *Sleep* *39*, 625–636. <https://doi.org/10.5665/sleep.5540>.
49. Lyamin, O.I., Pavlova, I.F., Kosenko, P.O., Mukhametov, L.M., and Siegel, J.M. (2012). Regional differences in cortical electroencephalogram (EEG) slow wave activity and interhemispheric EEG asymmetry in the fur seal. *J. Sleep Res.* *21*, 603–611. <https://doi.org/10.1111/j.1365-2869.2012.01023.x>.

50. Boyce, R., Glasgow, S.D., Williams, S., and Adamantidis, A. (2016). Causal evidence for the role of REM sleep theta rhythm in contextual memory consolidation. *Science* 352, 812–816. <https://doi.org/10.1126/science.aad5252>.
51. Girardeau, G., and Lopes-dos-Santos, V. (2021). Brain neural patterns and the memory function of sleep. *Science* 374, 560–564. <https://doi.org/10.1126/science.abi8370>.
52. Hahn, L.A., Balakhonov, D., Lundqvist, M., Nieder, A., and Rose, J. (2022). Oscillations without cortex: working memory modulates brainwaves in the endbrain of crows. *Prog. Neurobiol.* 219, 102372. <https://doi.org/10.1016/j.pneurobio.2022.102372>.
53. Raven, F., Van der Zee, E.A., Meerlo, P., and Havekes, R. (2018). The role of sleep in regulating structural plasticity and synaptic strength: Implications for memory and cognitive function. *Sleep Med. Rev.* 39, 3–11. <https://doi.org/10.1016/j.smrv.2017.05.002>.
54. Borbély, A.A., Tobler, I., and Hanagasioglu, M. (1984). Effect of sleep deprivation on sleep and EEG power spectra in the rat. *Behav. Brain Res.* 14, 171–182. [https://doi.org/10.1016/0166-4328\(84\)90186-4](https://doi.org/10.1016/0166-4328(84)90186-4).
55. Huber, R., Deboer, T., and Tobler, I. (2000). Effects of sleep deprivation on sleep and sleep EEG in three mouse strains: empirical data and simulations. *Brain Res.* 857, 8–19. [https://doi.org/10.1016/S0006-8993\(99\)02248-9](https://doi.org/10.1016/S0006-8993(99)02248-9).
56. Tobler, I., and Jaggi, K. (1987). Sleep and EEG spectra in the Syrian hamster (*Mesocricetus auratus*) under baseline conditions and following sleep deprivation. *J. Comp. Physiol. A* 161, 449–459. <https://doi.org/10.1007/BF00603970>.
57. Tobler, I., Franken, P., and Scherschlicht, R. (1990). Sleep and EEG spectra in the rabbit under baseline conditions and following sleep deprivation. *Physiol. Behav.* 48, 121–129. [https://doi.org/10.1016/0031-9384\(90\)90272-6](https://doi.org/10.1016/0031-9384(90)90272-6).
58. Güntürkün, O., Ströckens, F., and Ocklenburg, S. (2020). Brain lateralization: a comparative perspective. *Physiol. Rev.* 100, 1019–1063. <https://doi.org/10.1152/physrev.00006.2019>.
59. Rattenborg, N.C., Obermeyer, W.H., Vacha, E., and Benca, R.M. (2005). Acute effects of light and darkness on sleep in the pigeon (*Columba livia*). *Physiol. Behav.* 84, 635–640. <https://doi.org/10.1016/j.physbeh.2005.02.009>.
60. Mascetti, G.G., and Vallortigara, G. (2001). Why do birds sleep with one eye open? Light exposure of the chick embryo as a determinant of monocular sleep. *Curr. Biol.* 11, 971–974. [https://doi.org/10.1016/S0960-9822\(01\)00265-2](https://doi.org/10.1016/S0960-9822(01)00265-2).
61. Vallortigara, G., and Rogers, L.J. (2020). A function for the bicameral mind. *Cortex* 124, 274–285. <https://doi.org/10.1016/j.cortex.2019.11.018>.
62. Tommasi, L., Gagliardo, A., Andrew, R.J., and Vallortigara, G. (2003). Separate processing mechanisms for encoding of geometric and landmark information in the avian hippocampus. *Eur. J. Neurosci.* 17, 1695–1702. <https://doi.org/10.1046/j.1460-9568.2003.02593.x>.
63. Morandi-Raikova, A., and Mayer, U. (2021). Selective activation of the right hippocampus during navigation by spatial cues in domestic chicks (*Gallus gallus*). *Neurobiol. Learn. Mem.* 177, 107344. <https://doi.org/10.1016/j.nlm.2020.107344>.
64. Ulrich, C., Prior, H., Duka, T., Leshchins'ka, I., Valenti, P., Güntürkün, O., and Lipp, H.P. (1999). Left-hemispheric superiority for visuospatial orientation in homing pigeons. *Behav. Brain Res.* 104, 169–178. [https://doi.org/10.1016/S0166-4328\(99\)00062-5](https://doi.org/10.1016/S0166-4328(99)00062-5).
65. Gagliardo, A., Ioalè, P., Odetti, F., Bingman, V.P., Siegel, J.J., and Vallortigara, G. (2001). Hippocampus and homing in pigeons: left and right hemispheric differences in navigational map learning. *Eur. J. Neurosci.* 13, 1617–1624. <https://doi.org/10.1046/j.0953-816x.2001.01522.x>.
66. Lyamin, O.I., Kosenko, P.O., Korneva, S.M., Vyssotski, A.L., Mukhametov, L.M., and Siegel, J.M. (2018). Fur seals suppress REM sleep for very long periods without subsequent rebound. *Curr. Biol.* 28, 2000–2005.e2. <https://doi.org/10.1016/j.cub.2018.05.022>.
67. Tamaki, M., Bang, J.W., Watanabe, T., and Sasaki, Y. (2016). Night watch in one brain hemisphere during sleep associated with the first-night effect in humans. *Curr. Biol.* 26, 1190–1194. <https://doi.org/10.1016/j.cub.2016.02.063>.
68. Virtanen, P., Gommers, R., Oliphant, T.E., Haberland, M., Reddy, T., Cournapeau, D., Burovski, E., Peterson, P., Weckesser, W., Bright, J., et al. (2020). SciPy 1.0: fundamental algorithms for scientific computing in Python. *Nat. Methods* 17, 261–272. <https://doi.org/10.1038/s41592-019-0686-2>.
69. Harris, C.R., Millman, K.J., van der Walt, S.J., Gommers, R., Virtanen, P., Cournapeau, D., Wieser, E., Taylor, J., Berg, S., Smith, N.J., et al. (2020). Array programming with NumPy. *Nature* 585, 357–362. <https://doi.org/10.1038/s41586-020-2649-2>.
70. Hunter, J.D. (2007). Matplotlib: A 2D Graphics Environment. *Comput. Sci. Eng.* 9, 90–95. <https://doi.org/10.1109/MCSE.2007.55>.
71. Bates, D., Mächler, M., Bolker, B.M., and Walker, S.C. (2015). Fitting linear mixed-effects models using lme4. *J. Stat. Softw.* 67, 1–48. <https://doi.org/10.18637/jss.v067.i01>.
72. Wood, S.N. (2017). Generalized Additive Models: an Introduction with R, Second Edition (Chapman and Hall/CRC). <https://doi.org/10.1201/9781315370279>.
73. Lenth, R.V. (2016). Least-squares means: The R package lsmeans. *J. Stat. Softw.* 69, 1–33. <https://doi.org/10.18637/jss.v069.i01>.
74. Izawa, E.-I., and Watanabe, S. (2007). A Stereotaxic Atlas of the Brain of the Jungle Crow (*Corvus macrorhynchos*). *Integration of Comparative Neuroanatomy and Cognition*, 215–273.
75. Kersten, Y., Friedrich-Müller, B., and Nieder, A. (2022). A brain atlas of the carrion crow (*Corvus corone*). *J. Comp. Neurol.* 530, 3011–3038. <https://doi.org/10.1002/cne.25392>.
76. Stingelin, W. (1957). Vergleichend morphologische Untersuchungen am Vorderhirn der Vögel auf cytologischer und cytoarchitektonischer Grundlage (Helbing und Lichtenhahn Verlag).
77. Gramfort, A., Luessi, M., Larson, E., Engemann, D.A., Strohmeier, D., Brodbeck, C., Goj, R., Jas, M., Brooks, T., Parkkonen, L., et al. (2013). MEG and EEG data analysis with MNE-Python. *Front. Neurosci.* 7, 267.
78. RDC, T. (2010). A language and environment for statistical computing. Preprint.

STAR★METHODS

KEY RESOURCES TABLE

REAGENT or RESOURCE	SOURCE	IDENTIFIER
Experimental models: Organisms/strains		
European jackdaws (<i>Coloeus monedula</i>)	Retrieved from nest boxes in a wild colony	N/A
Software and algorithms		
RemLogic software	NeuroLite, Belp, Switzerland	https://neuroLite.ch/de/produkte/schlafmedizin/embla-remlogic-software
SciPy, version 1.2.1	Virtanen et al. ⁶⁸	https://docs.scipy.org/doc/scipy-1.2.1/reference/
Python libraries Numpy, version 1.26.4	Harris et al. ⁶⁹	https://numpy.org/devdocs/user/index.html
Matplotlib, version 3.9.2	Hunter ⁷⁰	
R software, lme4 package and mgcv package	Bates et al., ⁷¹ Wood, ⁷² and Lenth ⁷³	https://www.r-project.org , https://cran.r-project.org/web/packages/lme4/index.html , https://cran.r-project.org/web/packages/mgcv/index.html

EXPERIMENTAL MODEL AND STUDY PARTICIPANT DETAILS

Nine European jackdaws (5 males, 4 females) were used in this study. Pre-fledglings (30-day-old) were retrieved from nest boxes in a wild jackdaw colony. The jackdaws were group-housed in two seminatural enclosures, separated by gender. They were hand-fed 7 times a day between sunrise and sunset up to an age of 45 d (Versele-Laga, NutriBird A21, Deinze, België). During this time, they slowly acclimated to regular tap water from a tray and commercial food pellets (food item number 6659; Kasper Faunafood, Woerden, The Netherlands). The birds remained in the outdoor enclosures until an age of 10 months, when they underwent surgery for implantation of EEG electrodes. Two-weeks before the start of the experiments and EEG recordings, the animals were transferred indoors and were individually housed in cages (length = 74 cm, width = 87 cm, height = 97 cm). These cages contained an elevated stick where the birds could perch, and food and water were available ad libitum. Ambient temperature was kept constant at 21°C and there was a 12:12 LD-cycle with lights on from 8 am to 8 pm. Due to lighting and cage size, we were not able to record eye state in this study. All procedures were approved by the national Central Authority for Scientific Procedures on Animals (CCD) and the Institutional Animals Welfare Body (IvD, university of Groningen, The Netherlands).

METHOD DETAILS

Surgery

Before the surgery, meloxicam was injected subcutaneously as an analgesic (0.022 ml; 0.5 mg/kg) and diazepam was injected subcutaneously to reduce stress 10 min prior to surgery (0.09 ml; 2 mg/kg). Surgeries were performed under isoflurane anaesthesia (1.5–2%). After carefully exposing the crania, 30 holes with a diameter of 0.5 mm were drilled and rounded gold-plated electrode pins (0.5 mm diameter, BKL Electronic 10120538, Lüdenscheid, Germany) were inserted to the level of the dura mater. Twenty-eight electrodes were placed on the dorsal surface of the brain (14 on each hemisphere; Figure 1A). The distance between neighbouring electrodes was 4 mm. The remaining two electrodes were placed posteriorly to serve as a reference (4 mm posterior of the most posterior row of electrodes, on the midline near the anterior cerebellum) and a ground electrode (4 mm left of the reference electrode; Figure 1A). The 30 electrodes were soldered to a 32-channel connector (nanostrip connector A79028-001; Omnetics, Minneapolis, MN, USA) and the connector was secured to the head with Paladur dental cement (Heraeus Kulzer, Hanau, Germany). After surgery, the animals were allowed to recover for a minimum of two weeks before moving them to the indoor recording cages.

Although a brain atlas does not exist for the jackdaw, the gross anatomy of the brain is similar to that of jungle and carrion crows (*Corvus macrorhynchos* and *C. corone*, respectively) for which atlases exist.^{74–76} Based on these atlases, the anterior electrodes (rows 1–2, all columns) and the middle row (3, columns 1, 2, 5, and 6) were placed over the visual hyperpallium (Figure 1A).³² The posterior-medial electrodes were over the hippocampal formation (row 4, columns 3 and 4; row 5, columns 2–5),³³ and the posterior-lateral electrodes were over the DVR (rows 4 and 5; columns 1 and 6), a large structure that also extends under portions of the visual hyperpallium and hippocampal formation.³⁴ The exact boundary between the hyperpallium and hippocampal formation is histologically unclear in avian brain atlases. Also, the hippocampal formation thins laterally, where it overlies the lateral ventricle separating it from the underlying DVR. Consequently, the exact anterior and lateral boundaries of the hippocampal formation are poorly defined.

Sleep recordings

Before the start of the experiments, the jackdaws were extensively habituated to the indoor housing conditions and experimental procedures, including the mounting of the datalogger used for the sleep-wake recordings. The sleep-wake measurements were done by attaching a miniature datalogger to the head implant for recording EEG and head movement via accelerometry, with a total weight of 9.2 g (Neurologger 3; Evolocus, Tarrytown, NY, USA). The EEG and accelerometer data were sampled at 250 Hz and the logger could run for approximately 24 h on 1 rechargeable lithium polymer battery (165 mAh, 3.7 V; Renata, Itingen, Switzerland). The first-order high-pass filter set to 1 Hz in the logger recorded frequencies below 1 Hz with reduced amplitude (attenuation 20 dB/decade). We aimed to record sleep-wake patterns for three consecutive days, which meant that the batteries had to be replaced daily. This was done in the middle of the light phase, i.e., the active phase, to cause the least amount of disturbance to the normal sleep patterns. The 3-d recordings consisted of a baseline day, an experimental SD day, and an additional recovery day. Each of these days consisted of a full 12-h dark phase and subsequent light phase. All jackdaws underwent two 3-d recording sessions, during which they were subjected to two different durations of SD in a cross-over design. The birds were subjected to either 4- or 8-h of SD starting at lights off on the second day. Under low light, SD was achieved by means of 'mild stimulation' consisting of gently tapping the cage when birds showed signs of eye closure and inactivity. During the remainder of the second dark phase, subsequent light phase, and the third recording day, the animals could sleep undisturbed.

QUANTIFICATION AND STATISTICAL ANALYSIS

Data analyses

After the third recording day, the data was retrieved from the logger for sleep scoring. All recordings were coded and then scored by the same person (DM-G) blind to the experimental treatment and identity of the individual. Sleep scoring was done on the basis of all available EEG electrodes using RemLogic™ software (NeuroLite, Belp, Switzerland). Every 4-s epoch of the 3-d recording was assessed and labelled as either wake, NREM or REM sleep. Wake was scored whenever the recording showed high-frequency, low-amplitude EEG activity, often in combination with head movements visible in the accelerometer channels. NREM sleep was scored when the recording showed low-frequency, high-amplitude EEG activity, at least twice as high as the EEG amplitude during wakefulness in the majority of the channels for at least one hemisphere, together with a lack of head movements in the accelerometer channels. In practice, however, as shown in [Figure 1B](#), NREM usually started nearly synchronously within a hemisphere. NREM sleep was categorized as symmetric, asymmetric, or unihemispheric according to the criteria described below. REM sleep was scored when the NREM sleep pattern switched to low-amplitude, high-frequency EEG activity in each hemisphere, and without noticeable head movements in the accelerometer or sometimes with signs of head drops indicative of reduced muscle tone. However, we cannot rule out the possibility that some of the scored REM sleep included quiet wakefulness; although the reported amounts, bout durations, and timing of REM sleep were typical for other songbirds.⁴⁶ A bout of wakefulness, NREM sleep, or REM sleep, was considered a period uninterrupted by any other state.

The EEG data of all epochs scored as NREM sleep were further processed and subjected to power spectral density analysis for each 4-s epoch, based on a Discrete Fourier Transform and Welch's method (Hanning window of 500 samples, step size 100 samples), using SciPy version 1.2.1.⁶⁸ This yielded spectral power density values for 250 frequency bins (bin width: 0.5 Hz) up to a maximum of 125 Hz for all 28 EEG derivations. To correct for interindividual differences in the strength of the EEG signal, we expressed the spectral values of all 4-s NREM sleep epochs in all frequency bins relative to the mean spectral power in those same frequency bins during the baseline night.

We calculated a NREM sleep EEG asymmetry index for three intra-hemispheric electrode pairs. The 3 electrode pairs were 12 mm apart in a left to right axis (6 mm lateral of the midline) and 8 mm apart in an anterior-posterior axis ([Figure 4](#)). The asymmetry index has been used in several studies to calculate the strength and direction of the EEG asymmetry observed in NREM sleep in mammals⁴⁸ and birds.²⁵ We normalized the raw spectral NREM sleep EEG data of every electrode for every frequency bin relative to the mean night-time baseline levels of the same frequency bin of all EEG derivations of both hemispheres. We used averaged NREM sleep power for two frequency ranges that responded the most to SD (1.5 – 5.5 Hz SWA and the 7.5 – 18 Hz band). The asymmetry index was computed by $(\text{left hemisphere EEG power} - \text{right hemisphere EEG power}) / (\text{left hemisphere EEG power} + \text{right hemisphere EEG power})$.^{25,48} This yields a distribution ranging from -1 to +1 ([Figure 4A](#)). Symmetric NREM sleep is defined when the asymmetry index for 1.5 – 5.5 Hz SWA is between -0.33 and +0.33. Asymmetric NREM sleep is defined when the index lies between -0.67 and -0.33 or +0.33 and +0.67. All values lower than -0.67 and higher than +0.67 are considered unihemispheric NREM sleep.^{25,48} We used the same thresholds to categorize the level of inter-hemispheric asymmetry in 7.5 – 18 Hz power during NREM sleep. We further used the absolute asymmetry values to analyse the effects of SD on hemispheric asymmetry.

To visualize temporospatial patterns in electrical potentials across the electrode array, we created videos of EEG signals using the scientific Python libraries Numpy,⁶⁹ version 1.26.4, and Matplotlib,⁷⁰ version 3.9.2. We first filtered the raw EEG with a one-pass, zero-phase, non-causal 25-Hz low-pass filter, designed with the 'firwin' method (Hamming window) in MNE,⁷⁷ version 0.23.3, with a 53 dB stop band attenuation and a transition bandwidth of 6.25 Hz. Videos are slowed down by a factor 5 and have a frame rate of 50 Hz. This way, one frame in the video frame directly corresponds to one multi-channel EEG time sample (250 Hz), so there was no need for resampling in the time domain or other further conditioning.^{69,70,77}

Statistics

Data were analysed in R using linear mixed effect models as implemented by the lme4 package,^{71,78} with bird ID as a random effect. Whenever the random effect did not significantly contribute to the model, as assessed by using the likelihood-ratio test, a more simplistic linear regression model was computed. To assess the effect of SD on NREM sleep spectral power, we calculated the differences in NREM sleep EEG spectral power between the first hour after SD compared to the same hour during baseline up to 25 Hz for every EEG derivation and calculated the area under that curve. We modelled these changes in EEG power for all 28 derivations according to a generalized additive model (GAM) using the mgcv package.⁷² All post hoc analyses were done using the lsmeans package.⁷³ The absolute asymmetry index values were not normally distributed and were therefore log-transformed. Data in text and Figures 1, 2, and 4 are expressed as mean \pm SEM. Data in Figure 3 are expressed as mean \pm CI (95%).